Variational approach to light-matter interaction: Bridging quantum and semiclassical limits

Yiying Yan [1,*] Zhiguo Lü [2,†] and JunYan Luo [1]

[1] *Department of Physics, School of Science, Zhejiang University of Science and Technology, Hangzhou 310023, China*

[2] *Key Laboratory of Artificial Structures and Quantum Control (Ministry of Education), School of Physics and Astronomy, Shanghai Jiao Tong University, Shanghai 200240, China*

(Received 23 April 2024; accepted 2 July 2024; published 17 July 2024)

We present a time-dependent variational approach with the multiple-Davydov-D_2 trial state to simulate the dynamics of light-matter systems when the field is initially in a coherent state with an arbitrary finite mean photon number. The variational approach captures not only the system dynamics but also the field dynamics and is applicable to a variety of quantum models of light-matter interaction such as the Jaynes-Cummings model, Rabi model, and Dicke model and is capable of tackling multimode quantized fields. With a comparison of the variational and semiclassical dynamics of both the system and field, we illustrate that the variational dynamics from the quantum models agrees with those from the corresponding semiclassical models as long as the mean number of photons is sufficiently large. Moreover, we illustrate that in the crossover between the quantum and semiclassical limits, the quantum corrections lead to the collapse of the oscillations in dynamics, which is absent in the semiclassical models. The variational approach provides a unified treatment of light-matter interaction from the quantum to the semiclassical limit.

DOI: 10.1103/PhysRevA.110.013706

I. INTRODUCTION

Light-matter interaction between quantum systems and coherent fields plays a fundamental role in quantum optics [1,2], which enables control of the quantum system by the field or vice versa and is highly relevant to the realization of quantum technologies such as quantum information processing [3], quantum sensing [4,5], quantum metrology [6,7], and quantum batteries [8–11]. Theoretically, two kinds of descriptions of the light-matter interaction exist. One is based on the full quantum description with a quantized field. The other is based on the semiclassical description in which the field is treated classically. Two paradigmatic models for such theories are the quantum and semiclassical Rabi models [12–14]. Of particular interest, the study of these basic models has received renewed attention in artificial atoms. Both theoretical and experimental studies on the quantum Rabi model have been extended to the so-called ultrastrong-coupling regime [15–20], where the coupling constant becomes a considerable fraction of the field frequency. For the semiclassical Rabi model, strong driving with the Rabi frequency comparable to the transition frequency of the qubit can be achieved [21,22]. Such a strong-coupling (driving) regime has potential applications in the realization of ultrafast quantum gates [23,24].

Provided the field is initially in a coherent state, the quantum and semiclassical descriptions of light-matter interaction become consistent with each other in the semiclassical limit; that is, the mean photon number of the field tends to infinity, and the coupling constant tends to zero while their product remains constant [1,2,25]. However, in realistic situations, the quantum system can interact with only a finite number of photons rather than an infinite number of photons. A question naturally arises regarding under what conditions a finite number of photons cause a negligible deviation between the quantum and semiclassical models. Moreover, how quantum corrections in the presence of a finite number of photons contribute to the dynamics, which may be helpful in understanding the crossover between the quantum and semiclassical limits in particular, remains, to the best of our knowledge, barely explored.

Since fields are introduced in different ways in the quantum and semiclassical Hamiltonians, the light-matter interactions in the quantum and semiclassical limits are typically treated by different theoretical approaches. For instance, there are a variety of theoretical methods developed for the quantum Rabi model and its variants, e.g., the Van Vleck perturbation [26], unitary transformations [27–29], the variational approach [30–32], extended coherent states [33], etc. However, the Floquet theory mainly applies to semiclassical models [34,35]. In contrast to full quantum models, the field dynamics is ignored in semiclassical models. Very recently, a so-called photon-resolved Floquet theory was proposed to study the field dynamics of semiclassical models [36]. However, such an approach is established in the semiclassical limit and thus is inapplicable in the crossover between the quantum and semiclassical limits.

In this work, we present a unified numerical method that combines two sequential unitary transformations with a time-dependent variational approach equipped with the multiple-Davydov ansatz [37,38] to simulate the dynamics of light-matter systems from the quantum to semiclassical limit when the field is initially in a coherent state. One advantage of the variational approach is that the multiple-Davydov ansatz

*Contact author: yiyingyan@zust.edu.cn

†Contact author: zglv@sjtu.edu.cn

uses the coherent states as the bases, which effectively prevents the exponential increase in the size of the Hilbert space due to the increase in the number of modes and thus is applicable to a multimode case. More importantly, the variational approach simultaneously captures the dynamics of both the quantum system and fields. Particularly, we illustrate that the statistical characteristic function of the field can be computed, which allows us to calculate the mean value and variance of the photon numbers of the field as well as the photon-number distribution. We also show how the field dynamics can be calculated from semiclassical models. We apply the present approaches to a variety of light-matter systems, including the Jaynes-Cummings (JC) model, the Rabi model, and the Dicke model. By comparing the variational dynamics from the full quantum models with that from the semiclassical models, we examine the consistency between the quantum and semiclassical models in the presence of a large number of photons and illustrate the role of quantum corrections in the quantum-semiclassical crossover.

The rest of this paper is organized as follows. In Sec. II, we present the variational approach to treat the light-matter interaction in the presence of large mean photon numbers. We also show how to calculate the field dynamics in the semiclassical model. In Sec. III, we apply the variational approach and semiclassical approach to several light-matter systems and calculate the system and field dynamics. In Sec. IV, we draw our conclusions.

II. MODEL AND METHODS

The full quantum description of the interaction between a quantum system and a multimode coherent field can be described by the following Hamiltonian (we set $\hbar = 1$ throughout this work):

$$H = H_{\rm S} + \sum_{k=1}^{N} \omega_k b_k^\dagger b_k + \sum_{k=1}^{N} \frac{g_k}{2}(b_k^\dagger V_k + b_k V_k^\dagger), \tag{1}$$

where $H_{\rm S}$ is the free Hamiltonian of the quantum system and V_k is the interaction operator acting on the Hilbert space of the quantum system. b_k ($b_k^\dagger$) is the annihilation (creation) operator of the bosonic field with frequency ω_k. g_k is the coupling constant. N is the total number of modes. Note that either $V_k \neq V_k^\dagger$ or $V_k = V_k^\dagger$ is possible, corresponding to a rotating-wave approximation (RWA) and non-RWA Hamiltonian, respectively.

The time evolution of the composite system is governed by the time-dependent Schrödinger equation,

$$i\frac{d}{dt}|\Psi(t)\rangle = H|\Psi(t)\rangle, \tag{2}$$

where $|\Psi(t)\rangle$ is the state of the total system. In this work, we consider a factorized initial state of the total system

$$|\Psi(0)\rangle = |\psi(0)\rangle \otimes |\vec{\alpha}\rangle, \tag{3}$$

where $|\psi(0)\rangle$ is an initial state of the quantum system and $|\vec{\alpha}\rangle$ is a multimode coherent state that reads

$$\begin{aligned} |\vec{\alpha}\rangle &= |\alpha_1\rangle \otimes |\alpha_2\rangle \otimes \cdots \otimes |\alpha_N\rangle \\ &\equiv \exp\left(\sum_{k=1}^{N} \alpha_k b_k^\dagger - \text{H.c.}\right)|\mathbf{0}\rangle \equiv D(\vec{\alpha})|\mathbf{0}\rangle, \end{aligned} \tag{4}$$

where $|\mathbf{0}\rangle$ is a multimode vacuum state, $D(\vec{\alpha})$ is a displacement operator, and $\alpha_k \equiv |\alpha_k| e^{-i\phi_k}$ is a complex number with modulus $|\alpha_k|$ and phase ϕ_k.

A. Time-dependent variational approach

To achieve a manageable numerical simulation, we convert the time-evolution problem with the initial coherent state of a large number of photons into a new time-evolution problem with an initial vacuum state. This can be achieved with two sequential unitary transformations. First, we transform the time-dependent Schrödinger equation into the interaction picture governed by the free Hamiltonian of the field $H_{\rm F} = \sum_{k=1}^{N} \omega_k b_k^\dagger b_k$. In doing so, we have a new time-evolution problem:

$$i\frac{d}{dt}|\tilde{\Psi}(t)\rangle = \tilde{H}(t)|\tilde{\Psi}(t)\rangle, \tag{5}$$

where the Hamiltonian becomes time dependent,

$$\tilde{H}(t) = H_{\rm S} + \sum_{k=1}^{N} \frac{g_k}{2}(V_k^\dagger b_k e^{-i\omega_k t} + V_k b_k^\dagger e^{i\omega_k t}), \tag{6}$$

and the transformed wave function is related to the original one via

$$|\tilde{\Psi}(t)\rangle = \exp(iH_{\rm F}t)|\Psi(t)\rangle. \tag{7}$$

The initial state in the transformed frame remains the same as that in the original one, $|\tilde{\Psi}(0)\rangle = |\Psi(0)\rangle$. To proceed, we apply a displacement transformation to the equation of motion and the initial state, yielding

$$i\frac{d}{dt}|\Psi'(t)\rangle = H'(t)|\Psi'(t)\rangle, \tag{8}$$

where the displaced wave function is related to the original one via

$$|\Psi'(t)\rangle = D^\dagger(\vec{\alpha})\exp(iH_{\rm F}t)|\Psi(t)\rangle \tag{9}$$

and the transformed Hamiltonian is given by

$$\begin{aligned} H'(t) &= D^\dagger(\vec{\alpha})\tilde{H}(t)D(\vec{\alpha}) \\ &= H_{\rm S}(t) + \sum_{k=1}^{N} \frac{g_k}{2}(V_k^\dagger b_k e^{-i\omega_k t} + V_k b_k^\dagger e^{i\omega_k t}), \end{aligned} \tag{10}$$

where

$$H_{\rm S}(t) = H_{\rm S} + \sum_{k=1}^{N} \frac{\Omega_k}{2}[V_k e^{i(\omega_k t+\phi_k)} + V_k^\dagger e^{-i(\omega_k t+\phi_k)}], \tag{11}$$

$$\Omega_k = |\alpha_k| g_k. \tag{12}$$

In doing so, we have the following initial state:

$$|\Psi'(0)\rangle = D^\dagger(\vec{\alpha})|\Psi(0)\rangle = |\psi(0)\rangle|\mathbf{0}\rangle, \tag{13}$$

where the field is initially in the vacuum state in the transformed frame. Note that in the semiclassical limit of $g_k \to 0$ and $\alpha_k \to \infty$ but $|\alpha_k| g_k = \Omega_k$, the full quantum Hamiltonian of light-matter interaction becomes the semiclassical Hamiltonian, i.e., $H'(t) \to H_{\rm S}(t)$ [25].

We now use a time-dependent variational approach to compute the dynamics described by Eq. (8). The variational

approach is based on the Dirac-Frenkel time-dependent variational principle and the multiple-Davydov-D_2 ansatz. The former allows us to calculate the optimal solution to the time-dependent Schrödinger equation with a parameterized trial state. In this work, we use the multiple-Davydov-D_2 ansatz $|D_2^M(t)\rangle$, which is suitable for the spin-boson-like problems and is parameterized as follows [37–41]:

$$\left|D_2^M(t)\right\rangle = \sum_{n=1}^{M}\sum_{j=1}^{N_S} A_{nj}|j\rangle|f_n\rangle, \tag{14}$$

where M is the number of coherent states, A_{nj} are time-dependent variational parameters, $\{|j\rangle|j=1,2,\ldots,N_S\}$ represents a set of orthonormal bases for the quantum system, and

$$|f_n\rangle = \exp\left(\sum_{k=1}^{N} f_{nk}b_k^\dagger - \text{H.c.}\right)|\mathbf{0}\rangle \tag{15}$$

are multimode coherent states, with f_{nk} being time-dependent variational parameters. The equations of motion for variational parameters are determined by the Dirac-Frenkel time-dependent variational principle [42], that is,

$$\left\langle \delta D_2^M(t)\right|\left[i\partial_t - H'(t)\right]\left|D_2^M(t)\right\rangle = 0, \tag{16}$$

where $\langle \delta D_2^M(t)|$ represents the variation of the adjoint state. From Eq. (16), the equations of motion for the variational parameters are simply given by

$$i\langle j|\langle f_l\left|\dot{D}_2^M(t)\right\rangle = \langle j|\langle f_l|H'(t)\left|D_2^M(t)\right\rangle, \tag{17}$$

$$i\sum_{j=1}^{N_S} A_{lj}^*\langle j|\langle f_l|b_k\left|\dot{D}_2^M(t)\right\rangle = \sum_{j=1}^{N_S} A_{lj}^*\langle j|\langle f_l|b_k H'(t)\left|D_2^M(t)\right\rangle. \tag{18}$$

These equations of motion are a set of implicit first-order nonlinear differential equations and can be solved by the fourth-order Runge-Kutta algorithm [40,41]. A detailed derivation and implementation of the numerical simulation of Eqs. (17) and (18) are presented in the Appendix.

On solving the equations of motion, we can compute the quantities of interest for both the quantum system and the field. The observable of quantum system can be directly computed since the applied unitary transformations do not influence the operators acting on the Hilbert space of the matter system; e.g., the population of the state $|j\rangle$ can be given by

$$P_j(t) = \left\langle D_2^M(t)\right|j\rangle\langle j\left|D_2^M(t)\right\rangle = \sum_{l,n=1}^{M} A_{lj}^*\mathcal{S}_{ln}A_{nj}, \tag{19}$$

where

$$\mathcal{S}_{ln} = \exp\left[\sum_{k=1}^{N}\left(f_{lk}^* f_{nk} - \frac{|f_{lk}|^2}{2} - \frac{|f_{nk}|^2}{2}\right)\right]. \tag{20}$$

For the field, we calculate the moment-generating function,

$$\begin{aligned} G_{\vec{\chi}}(t) &= \left\langle e^{i\sum_{k=1}^{N}\chi_k b_k^\dagger b_k}\right\rangle_t \\ &= \left\langle D_2^M(t)\right|D^\dagger(\vec{\alpha})e^{i\sum_{k=1}^{N}\chi_k b_k^\dagger b_k}D(\vec{\alpha})\left|D_2^M(t)\right\rangle \\ &= \sum_{n,l=1}^{M}\sum_{j=1}^{N_S} A_{lj}^*\mathcal{S}_{ln}A_{nj} \\ &\quad\times\exp\left[\sum_{k=1}^{N}(e^{i\chi_k}-1)(\alpha_k^*+f_{lk}^*)(\alpha_k+f_{nk})\right], \end{aligned} \tag{21}$$

where $\chi_k \in [0, 2\pi)$, $\langle\cdot\rangle_t$ represents the average taken over the state in the laboratory frame, and we have used the identity of the displacement operators:

$$D(\alpha)D(\beta) = \exp\left(\frac{\alpha\beta^* - \alpha^*\beta}{2}\right)D(\alpha+\beta). \tag{22}$$

The moment-generating function contains the information of interest for the field. Particularly, the mean photon number in mode k can be computed as

$$\begin{aligned} n_k(t) &= \langle b_k^\dagger b_k\rangle_t = \frac{d}{id\chi_k}G_{\vec{\chi}}(t)|_{\chi_k=0} \\ &= \sum_{l,n=1}^{M}\sum_{j=1}^{N_S} A_{lj}^*\mathcal{S}_{ln}A_{nj}(\alpha_k^*+f_{lk}^*)(\alpha_k+f_{nk}). \end{aligned} \tag{23}$$

The variance of the photon number of mode k is given by

$$\sigma_k^2(t) = \frac{d^2}{i^2 d\chi_k^2}G_{\vec{\chi}}(t)|_{\chi_k=0} - n_k^2(t). \tag{24}$$

Additionally, the probability distribution of the photon numbers at time t can also be computed,

$$p(\vec{n},t) = \frac{1}{(2\pi)^N}\int_0^{2\pi} G_{\vec{\chi}}(t)e^{-i\vec{\chi}\cdot\vec{n}}d\vec{\chi}, \tag{25}$$

where $\vec{n} = (n_1, n_2, \ldots, n_N)$, with n_k being a non-negative integer that specifies the photon number of mode k.

B. Dynamics in the semiclassical limit

In this section, we compute the dynamics of the quantum system and field in the semiclassical limit. We first compute the population dynamics of the quantum system with Eq. (8). To this end, we express the time-evolution operator $U'(t) = \mathcal{T}\exp[-i\int_0^t H'(\tau)d\tau]$, with $\mathcal{T}$ being the time-ordering operator, by using the product form:

$$U'(t) = U_{\rm S}(t)U_{\rm I}'(t), \tag{26}$$

where

$$U_{\rm S}(t) = \mathcal{T}\exp\left[-i\int_0^t H_{\rm S}(\tau)d\tau\right] \tag{27}$$

is the time-evolution operator of the semiclassical Hamiltonian. $U_{\rm I}'(t)$ can be determined by iteration from the time-dependent Schrödinger equation and is readily given in terms of Dyson's series, which reads

$$\begin{aligned} U_{\rm I}'(t) &= 1 - i\int_0^t H_{\rm I}(\tau_1)d\tau_1 \\ &\quad - \int_0^t\int_0^{\tau_1} d\tau_1 d\tau_2 H_{\rm I}(\tau_1)H_{\rm I}(\tau_2) + \cdots, \end{aligned} \tag{28}$$

where

$$H_{\rm I}(t)=\sum_{k=1}^{N}\frac{g_k}{2}[V_k^{\dagger}(t)b_k e^{-i\omega_k t}+V_k(t)b_k^{\dagger}e^{i\omega_k t}], \tag{29}$$

$$V_k(t)=U_{\rm S}^{\dagger}(t)V_k U_{\rm S}(t). \tag{30}$$

With the above results at hand, we can calculate the population of the state $|j\rangle$ as follows:

$$P_j(t)=\langle\Psi'(t)|j\rangle\langle j|\Psi'(t)\rangle=\langle\Psi'(0)|U'^{\dagger}(t)|j\rangle\langle j|U'(t)|\Psi'(0)\rangle=P_j^{\rm sc}(t)+P_j^{\rm qc}(t), \tag{31}$$

with

$$P_j^{\rm sc}(t)=\langle\Pi_j(t)\rangle_0, \tag{32}$$

$$\begin{aligned}P_j^{\rm qc}(t)=&\sum_{k=1}^{N}\frac{g_k^2}{4}\int_0^t\int_0^t d\tau_1 d\tau_2\langle V_k^{\dagger}(\tau_1)\Pi_j(t)V_k(\tau_2)\rangle_0 e^{-i\omega_k(\tau_1-\tau_2)}\\&-{\rm Re}\sum_{k=1}^{N}\frac{g_k^2}{2}\int_0^t\int_0^{\tau_1}d\tau_1 d\tau_2\langle\Pi_j(t)V_k^{\dagger}(\tau_1)V_k(\tau_2)\rangle_0 e^{-i\omega_k(\tau_1-\tau_2)}+O\big(g_k^4\big),\end{aligned} \tag{33}$$

where $\langle\cdot\rangle_0$ represents the average taken over the initial state of the quantum system $|\psi(0)\rangle$ and

$$\Pi_j(t)=U_{\rm S}^{\dagger}(t)|j\rangle\langle j|U_{\rm S}(t). \tag{34}$$

In the above derivation, we have used the fact that the fields are in the vacuum state in the initial state $|\Psi'(0)\rangle$. Note that $P_j^{\rm sc}(t)$ is just the semiclassical dynamics, which is fully driven by the semiclassical Hamiltonian, that is,

$$\dot{U}_{\rm S}(t)=-iH_{\rm S}(t)U_{\rm S}(t). \tag{35}$$

$P_j^{\rm qc}(t)$ represents quantum corrections to the semiclassical dynamics, which is shown up to the second order in g_k. Clearly, there are higher-order corrections, which can be computed similarly. Such quantum corrections become vanishing in the limit of $g_k\to 0$, i.e., in the semiclassical limit.

Since in the semiclassical limit $|\alpha_k|\to\infty$, we calculate the change in the mean photon number of the mode k, which is simply given by

$$\Delta n_k(t)=\langle\Psi'(t)|D^{\dagger}(\vec{\alpha})(b_k^{\dagger}b_k-|\alpha_k|^2)D(\vec{\alpha})|\Psi'(t)\rangle=\langle\Psi'(0)|U'^{\dagger}(t)(b_k^{\dagger}b_k+\alpha_k^{*}b_k+\alpha_k b_k^{\dagger})U'(t)|\Psi'(0)\rangle. \tag{36}$$

Plugging Eq. (26) into (36), using the fact that the fields are in the vacuum state in the initial state $|\Psi'(0)\rangle$ and $U_{\rm S}(t)$ commutes with the field operators, and taking the semiclassical limit, we readily have

$$\Delta n_k(t)=-\Omega_k{\rm Re}\int_0^t i\langle V_k(\tau)\rangle_0 e^{i(\omega_k\tau+\phi_k)}d\tau. \tag{37}$$

Similarly, we can calculate the variance in the photon number of mode k:

$$\begin{aligned}\sigma_k^2(t)=&\langle\Psi'(t)|D^{\dagger}(\vec{\alpha})(b_k^{\dagger}b_k-|\alpha_k|^2)^2D(\vec{\alpha})|\Psi'(t)\rangle-\Delta n_k^2(t)=|\alpha_k|^2+\Delta n_k(t)-\Delta n_k^2(t)\\&+\frac{\Omega_k^2}{2}\int_0^t\int_0^t\langle V_k^{\dagger}(\tau_1)V_k(\tau_2)\rangle_0 e^{-i\omega_k(\tau_1-\tau_2)}d\tau_1 d\tau_2-\Omega_k^2{\rm Re}\int_0^t d\tau_1\int_0^{\tau_1}d\tau_2\langle V_k(\tau_1)V_k(\tau_2)\rangle_0 e^{i\omega_k(\tau_1+\tau_2)+2i\phi_k}.\end{aligned} \tag{38}$$

When $t=0$, one simply has $\sigma_k^2(0)=|\alpha_k|^2$, which is a feature of a coherent state. In practice, since $|\alpha_k|^2$ is a large number in the semiclassical limit, we subtract $|\alpha_k|^2$ from $\sigma_k^2(t)$ and calculate the change in the variance, i.e.,

$$\Delta\sigma_k^2(t)=\sigma_k^2(t)-|\alpha_k|^2. \tag{39}$$

This quantity characterizes the variation of the width of photon statistical distribution. Note that Eqs. (37) and (38) are justified only in the semiclassical limit $g_k\to 0$, $\alpha_k\to\infty$, and $g_k|\alpha_k|=\Omega_k$. In other words, they are inapplicable in the quantum and crossover regimes. As long as the semiclassical time-evolution operator is obtained, we can easily compute $\Delta n_k(t)$ and $\Delta\sigma_k^2(t)$. The time-evolution operator $U_{\rm S}(t)$ can be computed by directly integrating the time-dependent Schrödinger equation. Alternatively, it can be numerically or analytically computed with (generalized) Floquet theory.

III. APPLICATIONS

In this section, we apply the present variational approach and the semiclassical approach to study the dynamics of some light-matter systems. In doing so, we address the consistency between the quantum variational dynamics and semiclassical dynamics in the presence of a large number of photons and explore the role of quantum corrections. In the following calculations, the quantum system is assumed to be initially

in the ground state while the field is initially in a coherent state. Hereafter, the variational results will be denoted by "M-D_2," with M specifying a concrete number of coherent states used in simulations. The semiclassical results calculated from Eqs. (32), (37), and (39) are denoted by "SC" in the plots.

A. Jaynes-Cummings model

To begin with, we consider the JC model, the Hamiltonian of which reads

$$H = \frac{1}{2}\omega_0\sigma_z + \omega b^\dagger b + \frac{g}{2}(b\sigma_+ + b^\dagger\sigma_-), \tag{40}$$

where ω_0 is the transition frequency between two levels, $|1\rangle$ and $|2\rangle$, and $\sigma_z = |2\rangle\langle 2| - |1\rangle\langle 1|$ and $\sigma_+ = \sigma_-^\dagger = |2\rangle\langle 1|$. The notations for the field part are the same as in Eq. (1), and since there is a single mode, we have neglected the subscripts that label different modes for the field. This model and its semiclassical counterpart are exactly solvable, which provides transparent insights into the system and field dynamics as well as the quantum corrections to the semiclassical dynamics. For the quantized JC model, we use the variational approach to calculate the dynamics of the system and field. In the following, we introduce some analytical results from the semiclassical JC model.

The semiclassical Hamiltonian of the JC model is given by

$$H_S(t) = \frac{1}{2}\omega_0\sigma_z + \frac{\Omega}{2}(\sigma_+ e^{-i\omega t} + \sigma_- e^{i\omega t}). \tag{41}$$

The time-evolution operator reads [1]

$$U_S(t) = e^{-\frac{i\omega t\sigma_z}{2}}\left[\cos\left(\frac{\Omega_R t}{2}\right) - i\sin\left(\frac{\Omega_R t}{2}\right)\frac{\delta\sigma_z + \Omega\sigma_x}{\Omega_R}\right], \tag{42}$$

where $\delta = \omega_0 - \omega$ is the detuning and $\Omega_R = \sqrt{\Omega^2 + \delta^2}$ is the Rabi frequency. With the time-evolution operator and considering the initial state of the two-level system $|\psi(0)\rangle = |1\rangle$, we can easily obtain the excited-state population of the two-level system

$$P_2^{sc}(t) = \frac{\Omega^2}{\Omega_R^2}\sin^2\left(\frac{\Omega_R t}{2}\right). \tag{43}$$

This is the celebrated Rabi oscillation.

The change in photon number for the semiclassical JC model is obtained as

$$\Delta n(t) = -P_2^{sc}(t). \tag{44}$$

This means that the change in photon number and the excited-state population of the two-level system oscillate out of phase, which just reflects the conservation of the excitation number of the total system.

The change in the variance of the mean photon number is given by

$$\Delta\sigma^2(t) = \frac{(\Omega^2 - \delta^2)\Omega^2}{\Omega_R^4}\sin^2\left(\frac{\Omega_R t}{2}\right) - \frac{\Omega^4}{\Omega_R^4}\sin^4\left(\frac{\Omega_R t}{2}\right) - \frac{\Omega^4 t}{2\Omega_R^3}\sin(\Omega_R t). \tag{45}$$

The above analytical results for the field part are obtained in the semiclassical limit, and quantum corrections are not involved.

We now address how the deviation in the dynamics between the quantum and semiclassical JC model emerges due to the variation of the the initial mean numbers of photons by comparing the variational and analytical results. In Fig. 1, we show the dynamics of the system and field by computing the excited-state population $P_2(t)$, the change in photon number $\Delta n(t)$, and the change in variance of the photon number $\Delta\sigma^2(t)$ from the quantum and semiclassical JC models for $\omega = \omega_0$. For the quantum model, we consider three values of the initial mean number of photons α^2 ranging from 10^5 to 10^3. The coupling constant and the Rabi frequency are set by $g\alpha = \Omega = 0.5\omega_0$. Figures 1(a)–1(c) show that when $\alpha^2 = 10^5$, the quantum and semiclassical dynamics for either the system or field are in perfect agreement in the time interval, indicating the consistency between the quantum and semiclassical models in the large-mean-photon-number limit. Figures 1(d)–1(f) show that when $\alpha^2 = 10^4$, the quantum variational dynamics and the semiclassical dynamics are almost the same when $t < 200\omega_0^{-1}$, while they deviate from each other when $t > 200\omega_0^{-1}$. Moreover, Figs. 1(g)–1(i) show that when $\alpha^2 = 10^3$, the quantum variational dynamics just coincides with the semiclassical dynamics in the first few cycles of the Rabi oscillation. As time goes on, one readily notes that for full quantum dynamics, the Rabi oscillation in the population of the system experiences a significant collapse, which is a quantum feature and is absent in the semiclassical limit [1,43]. The striking difference between the quantum and semiclassical results reflects the role of quantum corrections to the semiclassical dynamics in the quantum-semiclassical crossover.

To provide a criterion for assessing the timescale within which the quantum and semiclassical models yield consistent dynamics, we further explore the role of the quantum corrections. We calculate the difference between the variational population dynamics $P_2(t)$ and the semiclassical dynamics $P_2^{sc}(t)$, which is just the "exact" quantum correction. Alternatively, we can calculate the quantum correction up to the second order in g for the JC model. It follows from Eqs. (33) and (42) that the second-order quantum correction to the semiclassical population dynamics is given by

$$P_2^{qc}(t) = \frac{g^2\Omega^2}{4\Omega_R^4}\left\{\frac{\Omega^2 t^2}{4}\cos(\Omega_R t) + \frac{4\delta^2 - \Omega^2}{4\Omega_R}t\sin(\Omega_R t) - \frac{4\delta^2}{\Omega_R^2}\sin^2\left(\frac{\Omega_R t}{2}\right)\right\}. \tag{46}$$

The analytical result shows that the amplitude of oscillation is proportional to t^2. This means that even if g is a small quantity, the quantum correction can contribute significantly to the long-time limit. Moreover, this result is ill defined as $t \to \infty$, suggesting that the second-order quantum correction to the semiclassical dynamics is insufficient in the quantum-semiclassical crossover and higher-order quantum corrections must be involved. In Fig. 2, we plot the numerically exact and second-order quantum corrections as a function of time t for $\alpha^2 = 10^4$, $\Omega = g\alpha = 0.5\omega_0$, and $\omega = \omega_0$. One readily finds that the second-order quantum correction plays a

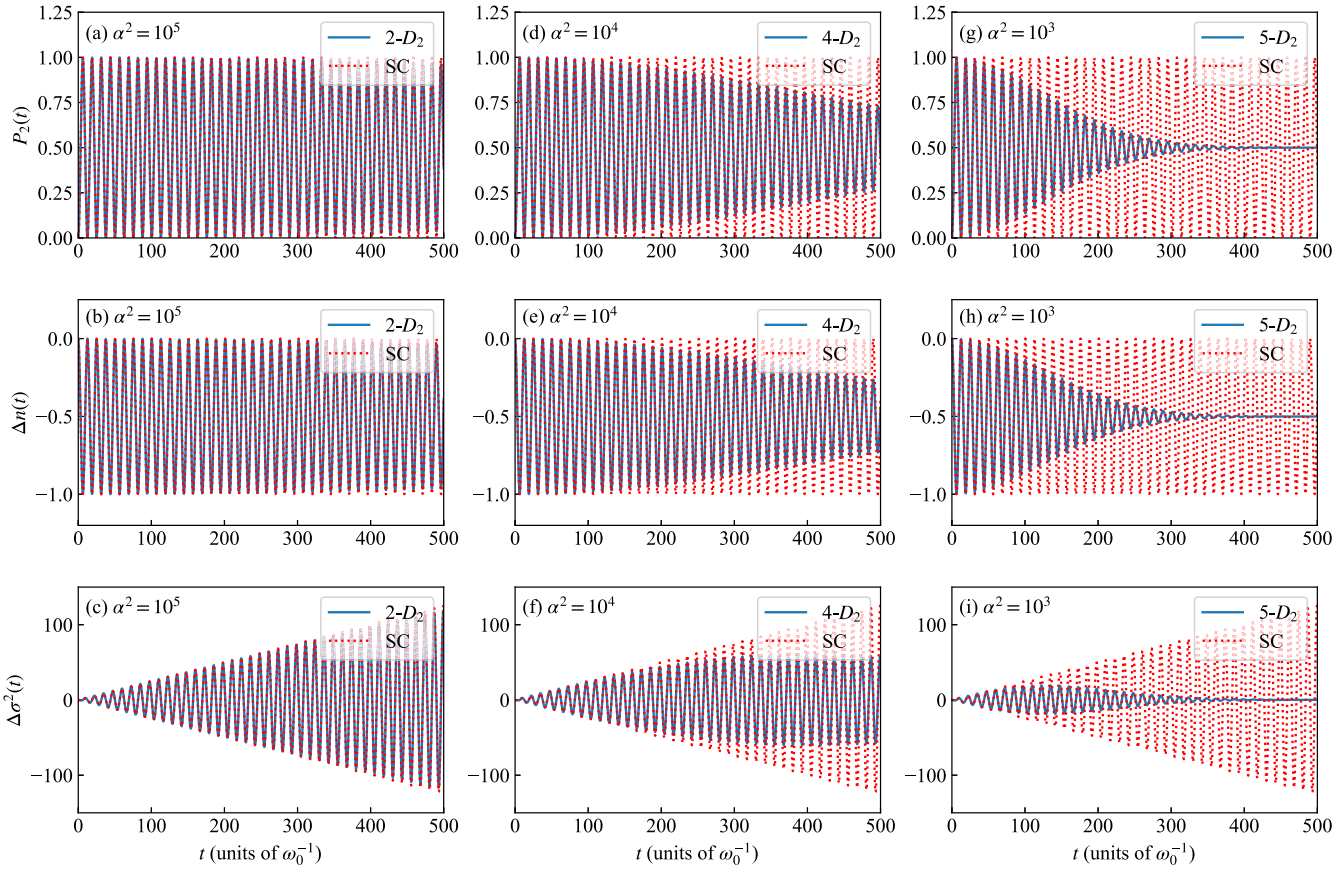

FIG. 1. Excited-state population $P_2(t)$, change in photon number $\Delta n(t)$, and change in the variance of the photon number $\Delta\sigma^2(t)$ calculated by the quantum variational approach and semiclassical approach for the quantum and semiclassical JC models. For the semiclassical model, the parameters are set as $\Omega = 0.5\omega_0$ and $\omega = \omega_0$. For the quantum model, $g\alpha = \Omega$, $\omega = \omega_0$, and three values of the initial mean photon number α^2 are used. "2-D_2" denotes the variational results with $M = 2$. "SC" denotes the semiclassical results.

predominant role and agrees with the exact one in the finite-time interval. This finding actually can be used to estimate the upper bound of time t_c below which the quantum dynamics and semiclassical dynamics are consistent. Roughly speaking, we require $g^2 t_c^2 < 1$ such that the second-order correction is a small quantity. Using $g = \Omega/|\alpha|$, we have $t_c < |\alpha|/\Omega$; that is, the larger the mean photon number is, the more the quantum and semiclassical dynamics coincide with each other over a longer time interval. For instance, when considering the parameters in Fig. 1(c), we find that $t_c \approx 63\omega_0^{-1}$, which turns out to be a good estimation of the timescale.

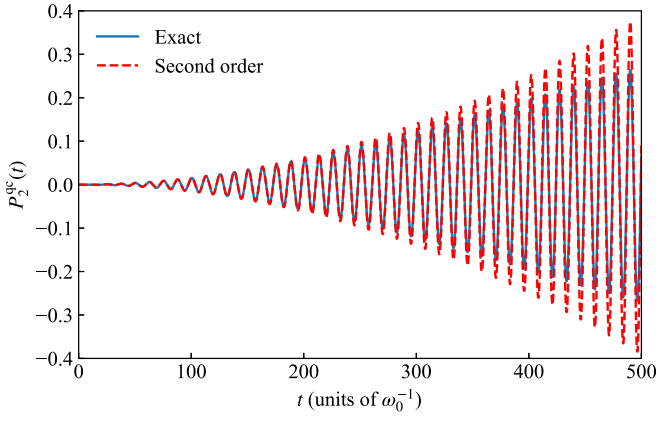

FIG. 2. Exact and second-order quantum corrections to the excited-state population of the qubit in the JC model for $\Omega = g\alpha = 0.5\omega_0$, $\omega = \omega_0$, and $\alpha^2 = 10^4$. The exact quantum correction is obtained as the difference between the quantum dynamics $P_2(t)$ and the semiclassical dynamics $P_2^{sc}(t)$. The second-order quantum correction is given by Eq. (46).

The present variational approach can also be used to calculate the photon-number distribution at given times. Figures 3(a)–3(c) show $p(n,t)$ as a function of n at two given times for $\omega = \omega_0$, $g = 0.5\omega_0/\alpha$, and three values of α. When $t = 0$, the photon-number distribution is the Poisson distribution peaking at $n = |\alpha|^2$, which is the nature of the coherent state. When $\alpha^2 = 10^5$ or 10^4, we see that there is almost no difference between the initial ($t = 0$) and final ($t = 500\omega_0^{-1}$) photon-number distributions. This finding is consistent with the results in Figs. 1(c) and 1(f), where one finds that although the oscillation amplitude of the change in the variance of photon number $\Delta\sigma^2(t)$ increases with time t, its magnitude is far smaller than the initial variance $\sigma^2(0) = \alpha^2$, i.e., $\Delta\sigma^2(t) \ll \sigma^2(0)$. Consequently, the width of the photon-number distribution hardly changes in the semiclassical limit. However, when $\alpha^2 = 10^3$, Fig. 3(c) shows that the final photon-number distribution is different from the initial one. The present results suggest that the photon-number distribution rarely changes in the semiclassical limit but can change due to the

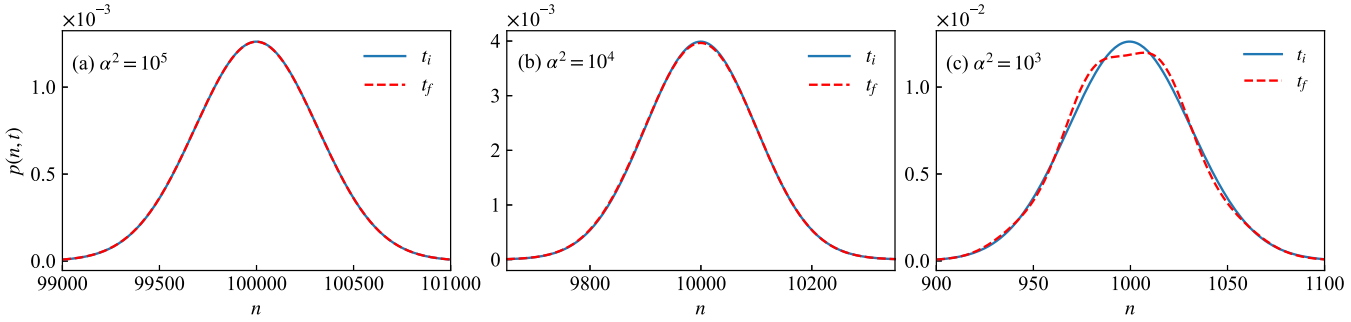

FIG. 3. Photon-number distribution $p(n,t)$ as a function of the photon number n at the two given times calculated by the variational approach for $\Omega = g\alpha = 0.5\omega_0$, $\omega = \omega_0$, and three values of α^2. t_i and t_f denote the initial time $t = 0$ and finial time $t = 500\omega_0^{-1}$, respectively.

light-matter interaction in the crossover region between the quantum and semiclassical limits.

The present results suggest that the variational approach is applicable to light-matter systems not only in the quantum limit [31] but also in the semiclassical limit, as well as the crossover in between, and is capable of tackling a relatively large mean number of photons. On the other hand, the present results confirm that field dynamics can also be calculated in the semiclassical model.

B. Rabi model

1. Single-mode case

The JC model may be inadequate due to the RWA, and we move to consider the quantum Rabi model, the Hamiltonian of which reads

$$H = \frac{1}{2}\omega_0\sigma_z + \omega b^\dagger b + \frac{g}{2}(b + b^\dagger)\sigma_x, \tag{47}$$

where $\sigma_x = \sigma_+ + \sigma_-$. We apply the variational approach to study the dynamics of the quantum Rabi model. We also calculate the semiclassical dynamics of the system and field, which is based on the numerically calculated time-evolution operator for the semiclassical Rabi model: $H_S(t) = \frac{1}{2}\omega_0\sigma_z + \Omega\cos(\omega t)\sigma_x$.

We examine the consistency between the variational dynamics and the semiclassical dynamics under the initial condition of a large number of photons, i.e., $\alpha^2 \gg 1$. In Fig. 4, we show the dynamics of the excited-state population $P_2(t)$, the change in photon number $\Delta n(t)$, and the change in the variance of the mean photon number $\Delta\sigma^2(t)$ for the quantum and semiclassical Rabi models. We consider three values of α^2 and $\omega = \omega_0$. The Rabi frequency and coupling constant are given by $\Omega = 0.5\omega_0$ and $g = \Omega/\alpha$, respectively. We note that the quantum variational dynamics and semiclassical dynamics are almost the same when $\alpha^2 = 10^5$. However, when $\alpha^2 = 10^4$ or 10^3, the difference between the variational and semiclassical dynamics appears as time increases, which is attributed to the quantum corrections to the semiclassical dynamics. This situation is similar to that encountered in the JC model. In addition, we note that there are beat behaviors in Fig. 4 which result from the counterrotating terms [34,44,45]. To explore the validity of the variational approach in the quantum limit, we calculate the dynamics of the system and field for the quantum Rabi model by using the variational approach and the numerically exact diagonalization (ED) of the quantum Rabi Hamiltonian for $\omega = \omega_0$, $g = 0.2\omega_0$, and $\alpha^2 = 5$. Since $g = 0.2\omega_0$ is comparable to ω, the light-matter coupling is ultrastrong. This is a regime where the two-level system ultrastrongly interacts with a few photons, and thus, the semiclassical approach is inapplicable. Figure 5 shows that in comparison with the ED method, the variational approach can produce accurate dynamics of the system and field, as well as the photon-number distribution, for the quantum Rabi model in an ultrastrong-coupling regime. The present findings suggest that the variational approach provides a unified method to tackle light-matter systems in both the quantum and semiclassical limits. More importantly, it captures the dynamics of both the system and field. This is of particular importance in potential applications for studying the statistical properties of the field.

2. Two-mode case

We now exploit the developed formalisms to study the system and field dynamics in the two-mode cases, where multiphoton processes become remarkable. The Hamiltonian of the two-mode quantum Rabi model is given by

$$H = \frac{\omega_0}{2}\sigma_z + \sum_{k=1}^{N}\omega_k b_k^\dagger b_k + \sum_{k=1}^{N}\frac{g_k}{2}(b_k + b_k^\dagger)\sigma_x, \tag{48}$$

where the number of modes is $N = 2$. The Hamiltonian of the two-mode semiclassical Rabi model is given by

$$H_S(t) = \frac{\omega_0}{2}\sigma_z + [\Omega_1\cos(\omega_1 t) + \Omega_2\cos(\omega_2 t)]\sigma_x, \tag{49}$$

which describes a bichromatically driven two-level system. As is well known, the two-level system may absorb $n+1$ photons from one field and emit n photons into the other field, which can lead to multiphoton resonances occurring at $\omega_0 \approx (n+1)\omega_1 - n\omega_2$, with n being an integer. Such multiphoton resonances have been studied in the semiclassical model with and without the RWA [46–50] and are illustrated by calculating the transition probabilities of the two-level system. Here we revisit this phenomenon by calculating not only the population of the system but also the photon-number dynamics by making use of variational and semiclassical approaches. In the latter approach, the time-evolution operator of the semiclassical model is numerically calculated using the Runge-Kutta method.

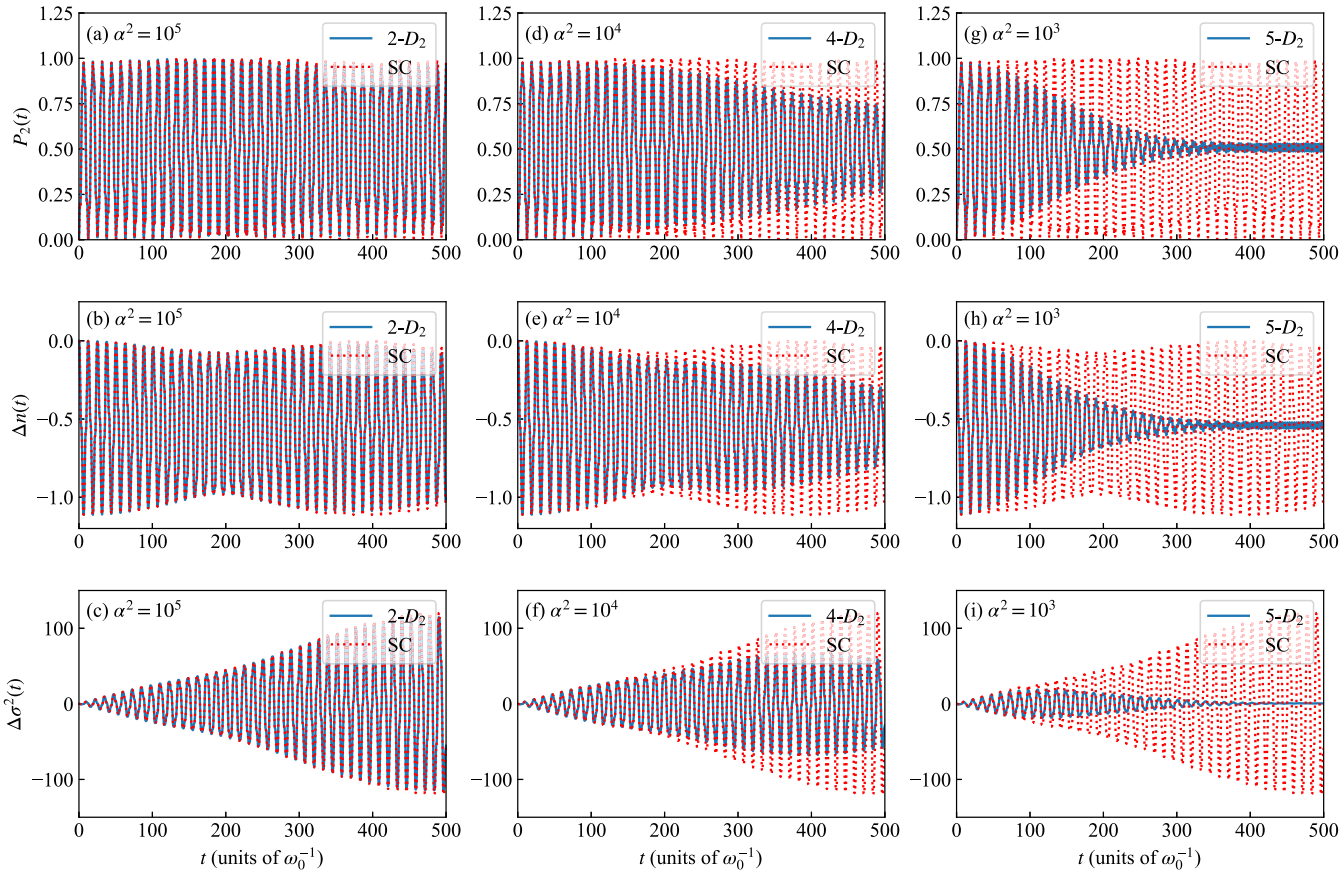

FIG. 4. Excited-state population $P_2(t)$, change in photon number $\Delta n(t)$, and change in the variance of the photon number $\Delta\sigma^2(t)$ calculated by the quantum variational approach and semiclassical approach for the quantum and semiclassical Rabi models. For the semiclassical model, the parameters are set as $\Omega = 0.5\omega_0$ and $\omega = \omega_0$. For the quantum model, $g\alpha = \Omega$, $\omega = \omega_0$, and three values of the initial mean photon number α^2 are used.

The multiphoton resonance condition can be numerically obtained with the generalized Floquet theory [47]. To be concrete, we consider $\omega_1 = 0.6449\omega_0$, $\omega_2 = 0.8449\omega_0$, and $\Omega_1 = \Omega_2 = 0.3\omega_0$ for the semiclassical model, which corresponds to a resonance in which the two-level system absorbs two photons from mode 2 and emits one photon into mode 1. For the quantized field, we set $g_1 = g_2 = 0.3\omega_0/\alpha$ and $\alpha_1^2 = \alpha_2^2 = \alpha^2 = 10^5$. In Figs. 6(a)–6(c), we depict the excited-state population $P_2(t)$, the change in photon number $\Delta n_k(t)$, and the change in the variance $\Delta\sigma_k^2(t)$ for the quantum and semiclassical models. It is evident that the dynamics of the system and fields from the quantum model are in agreement with those from the semiclassical model, confirming that the variational approach can be applied to simulate the semiclassical dynamics in the two-mode cases, provided the initial mean photon number is sufficiently large. In Fig. 6(a), we see

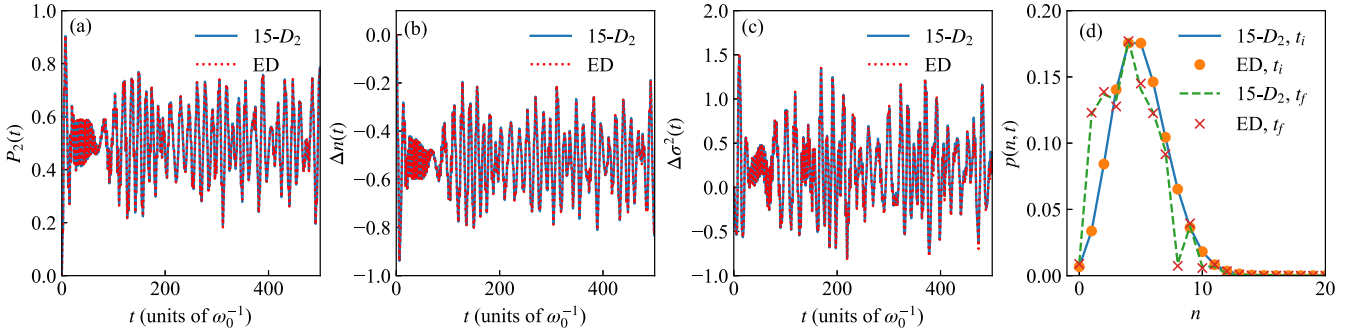

FIG. 5. (a) Excited-state population $P_2(t)$, (b) change in photon number $\Delta n(t)$, (c) change in the variance of the photon number $\Delta\sigma^2(t)$, and (d) photon-number distribution $p(n,t)$ calculated by the variational approach and numerically exact diagonalization (ED) for the quantum Rabi model. The parameters are set as $g = 0.2\omega_0$, $\omega = \omega_0$, and $\alpha^2 = 5$. t_i and t_f in (d) denote the initial time $t = 0$ and finial time $t = 500\omega_0^{-1}$, respectively.

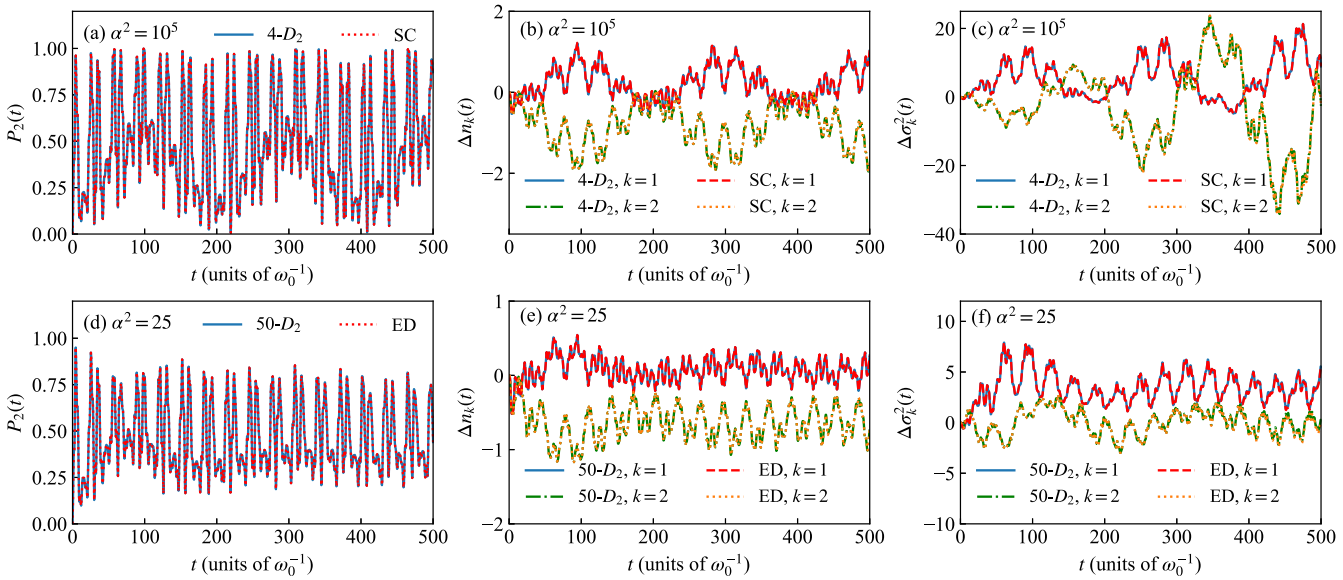

FIG. 6. Excited-state population $P_2(t)$, change in photon number $\Delta n_k(t)$, and change in the variance of the photon number $\Delta\sigma_k^2(t)$ calculated by the variational approach, (a)–(c) the semiclassical approach, and (d)–(f) the ED method for the two-mode quantum and semiclassical Rabi models. For the semiclassical model, the parameters are set as $\omega_1 = 0.6449\omega_0$, $\omega_2 = 0.8449\omega_0$, and $\Omega_1 = \Omega_2 = 0.3\omega_0$. For the quantum model, $\omega_1 = 0.6449\omega_0$, $\omega_2 = 0.8449\omega_0$, $g_1 = g_2 = \Omega_1/\alpha$, and $\alpha_1 = \alpha_2 = \alpha$. Two values of the initial mean photon number α^2 are used.

that the excited-state population can reach a maximum value $P_2(t) = 1$, which signifies the occurrence of a resonance. In Fig. 6(b), the change in photon numbers in the two modes manifests the multiphoton feature of the resonance.

Figures 6(d)–6(f) show the dynamics of the system and fields for the model with quantized fields in the case of $\alpha_1^2 = \alpha_2^2 = \alpha^2 = 25$ and $g_1 = g_2 = \Omega_1/\alpha = 0.06\omega_0$. Comparisons between the variational results and those of the ED method confirm that the variational approach is applicable in the quantum limit in the two-mode case. In addition, we see that the system and field dynamics in the case of $\alpha^2 = 25$ are apparently different from those in the case of $\alpha^2 = 10^5$. Specifically, the excited-state population cannot reach a maximum value $P_2(t) = 1$ in the former case, indicating the disappearance of the multiphoton resonance due to the quantum corrections. In Figs. 7(a) and 7(b), we compare the photon-number distribution $p(\vec{n}, t)$, with $\vec{n} = (n_1, n_2)$, at $t = 500\omega_0^{-1}$ calculated from the variational and ED methods for the same parameters as in Figs. 6(d)–6(f). The two methods predict almost the same photon-number distribution, which is apparently different from the initial two-dimensional Poisson distribution due to the strong light-matter coupling.

C. Dicke model

In this section, we consider the Dicke model [51], which is described by the following Hamiltonian:

$$H = \omega b^\dagger b + \frac{1}{2}\sum_{j=1}^{N_q}[\omega_{0,j}\sigma_{z,j} + g(b + b^\dagger)\sigma_{x,j}], \tag{50}$$

where N_q is the number of two-level systems, $\omega_{0,j}$ is the transition frequency of the jth two-level system, and $\sigma_{\mu,j}$ is the Pauli matrix for the jth two-level system. The semiclassical counterpart of the Dicke model is given by

$$H_S(t) = \sum_{j=1}^{N_q}\left[\frac{1}{2}\omega_{0,j}\sigma_{z,j} + \Omega\cos(\omega t)\sigma_{x,j}\right]. \tag{51}$$

Figure 8 shows the change in photon number $\Delta n(t)$ calculated by the variational and semiclassical approaches for $N_q = 2$, $\omega = \omega_{0,1}$, $\Omega = 0.5\omega_{0,1}$, and three values of $\omega_{0,2}$. For the quantum model, we consider two values of α^2 and $g = \Omega/\alpha$. In Figs. 8(a)–8(c), we see that when $\alpha = 10^5$, the variational quantum dynamics coincides with the semiclassical dynamics. Figures 8(d)–8(f) show that when $\alpha^2 = 10^3$, the oscillation from the quantum model undergoes collapse. The present results on the consistency between the quantum and semiclassical models are similar to those for the JC and Rabi models.

Figure 8 also provides insights into how the field responds due to the presence of multiple two-level systems. When the two-level systems are identical, i.e., $\omega_{0,2} = \omega_{0,1}$, the photon number dynamics is similar to that of the Rabi model shown in Fig. 4(b), except that the amplitude of the oscillation is about 2, which reflects the fact that the two photons can be absorbed by the two subsystems. On the other hand, when the two-level systems have different transition frequencies, there are strong beat behaviors that can be tuned by the frequency difference in the two subsystems, which result from the two independent Rabi oscillations of the two subsystems that have different Rabi frequencies.

IV. CONCLUSIONS

In summary, we presented a time-dependent variational approach to study the system and field dynamics of light-matter systems when the field is initially in a coherent state and possesses a finite mean number of photons. In

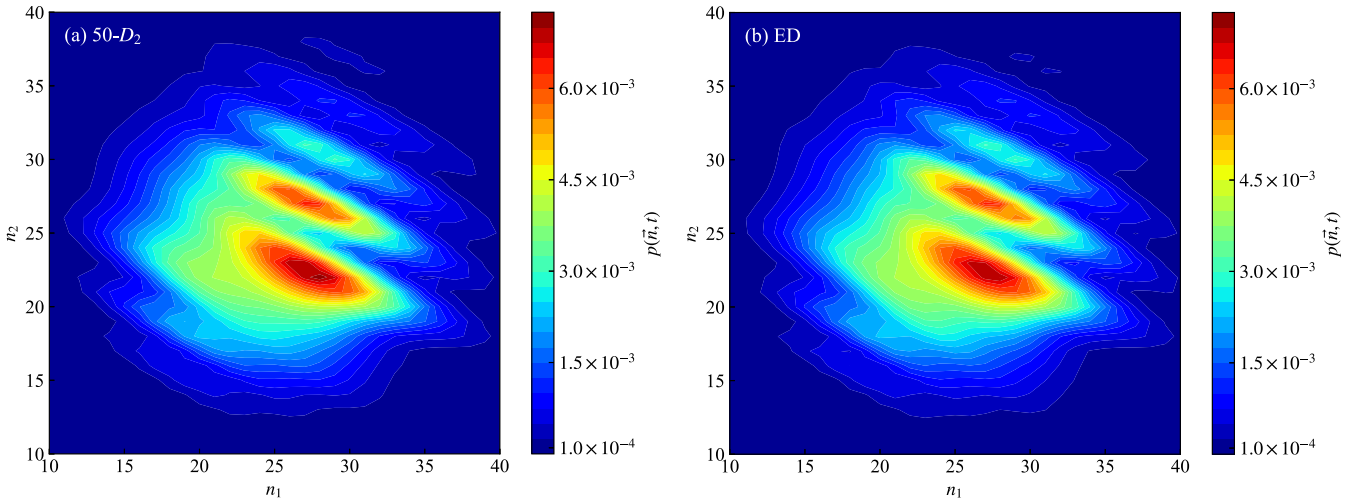

FIG. 7. Photon-number distribution $p(\vec{n},t)$ with $\vec{n}=(n_1,n_2)$ at $t=500\omega_0^{-1}$ for the two-mode quantum Rabi model calculated by (a) the variational approach and (b) the ED method. The parameters are the same as in Fig. 6(d).

addition to the variational approach, we showed that the field dynamics can also be deduced from the system dynamics in the semiclassical model. By using the variational and semiclassical approaches, we examined the consistency in the system and field dynamics between the quantum and semiclassical models of light-matter interaction in the large-mean-photon-number regimes. We illustrated that the variational approach can produce accurate semiclassical dynamics of either the system or the field as long as the initial mean photon number is sufficiently large. Moreover, it can also produce accurate quantum dynamics of the system and field when a few photons strongly interact with the quantum system and can apply to the crossover between the quantum and semiclassical limits. In the crossover region, we showed that the excited-state population of the quantum system and the change in photon number experience a collapse in the amplitude of the oscillations, which reflects the quantum nature. The present variational approach provides a unified treatment of light-matter interaction in the quantum and semiclassical limits as well as the crossover in between.

The variational approach can also be extended to open quantum systems based on two routines. One is that the dissipation is taken into account by considering a set of harmonic oscillators to be the environment such as the well-known spin-boson model [38,52]. The other is that the dissipation is modeled by non-Hermitian Hamiltonians. The variational approach with the Davydov ansatz can be extended to solve the time-dependent Schrödinger equation with a non-Hermitian Hamiltonian. This has the potential to describe cavity-QED systems with a lossy cavity.

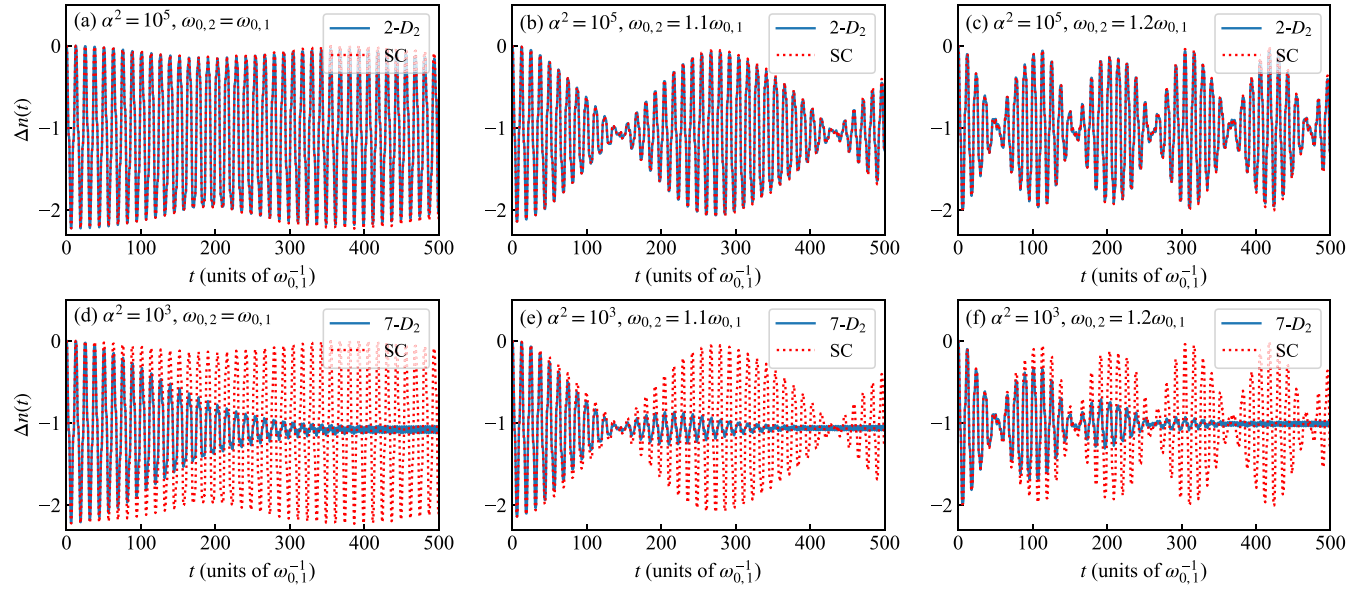

FIG. 8. Change in photon number $\Delta n(t)$ calculated by the variational approach and semiclassical approach for the two-qubit Dicke model and its semiclassical counterpart with $N_q=2$. For the semiclassical model, $\Omega=0.5\omega_{0,1}$, $\omega=\omega_{0,1}$, and three values of $\omega_{0,2}$ are used. For the quantum model, $g\alpha=\Omega$, two values of the initial mean photon number α^2 are used, and the other parameters are the same as in the semiclassical model.

ACKNOWLEDGMENT

Support from the National Natural Science Foundation of China (Grants No. 12005188, No. 11774226, and No. 11774311) is gratefully acknowledged.

APPENDIX: THE EQUATIONS OF MOTION FOR THE VARIATIONAL PARAMETERS AND NUMERICAL IMPLEMENTATION

The variation of the joint state of $|D_2^M(t)\rangle$ is given by

$$\left\langle \delta D_2^M(t)\right| = \sum_{l=1}^{M}\sum_{j=1}^{N_S}\langle j|\langle f_l|\left\{\delta A_{lj}^* + A_{lj}^*\sum_{k=1}^{N}\left[\delta f_{lk}^*\left(b_k - \frac{1}{2}f_{lk}\right) - \frac{1}{2}\delta f_{lk}f_{lk}^*\right]\right\}. \tag{A1}$$

Substituting $\langle \delta D_2^M(t)|$ into Eq. (16), we simply derive

$$\begin{aligned} 0 = &\sum_{l=1}^{M}\sum_{j=1}^{N_S}\delta A_{lj}^*\langle j|\langle f_l|[i\partial_t - H'(t)]\left|D_2^M(t)\right\rangle + \sum_{l=1}^{M}\sum_{k=1}^{N}\delta f_{lk}^*\sum_{j=1}^{N_S}A_{lj}^*\langle j|\langle f_l|\left(b_k - \frac{1}{2}f_{lk}\right)[i\partial_t - H'(t)]\left|D_2^M(t)\right\rangle \\ &- \sum_{l=1}^{M}\sum_{j=1}^{N_S}A_{lj}^*\sum_{k=1}^{N}\frac{\delta f_{lk}f_{lk}^*}{2}\langle j|f_l|[i\partial_t - H'(t)]\left|D_2^M(t)\right\rangle. \end{aligned} \tag{A2}$$

To ensure the above equation holds for arbitrary variation of the parameters, we simply have

$$\langle j|\langle f_l|[i\partial_t - H'(t)]\left|D_2^M(t)\right\rangle = 0, \tag{A3}$$

$$\sum_{j=1}^{N_S}A_{lj}^*\langle j|\langle f_l|\left(b_k - \frac{1}{2}f_{lk}\right)[i\partial_t - H'(t)]\left|D_2^M(t)\right\rangle = 0. \tag{A4}$$

Equation (A3) corresponds to Eq. (17) in the main text and can be used to simplify Eq. (A4), which leads to Eq. (18) in the main text.

To derive the explicit forms of the equations of motion, we use the time derivative of the trial state [40]

$$\left|\dot{D}_2^M(t)\right\rangle = \sum_{n=1}^{M}\sum_{i=1}^{N_S}\left[a_{ni} + A_{ni}\sum_{p=1}^{N}\dot{f}_{np}b_p^\dagger\right]|i\rangle|f_n\rangle, \tag{A5}$$

where

$$a_{ni} = \dot{A}_{ni} - \frac{1}{2}A_{ni}\sum_{p=1}^{N}(\dot{f}_{np}f_{np}^* + f_{np}\dot{f}_{np}^*). \tag{A6}$$

To proceed, we carry out a calculation for $\langle j|\langle f_l|\dot{D}_2^M(t)\rangle$, $\sum_{j=1}^{N_S}A_{lj}^*\langle j|\langle f_l|b_k|\dot{D}_2^M(t)\rangle$, $\langle j|\langle f_l|H'(t)|D_2^M(t)\rangle$, and $\sum_{j=1}^{N_S}A_{lj}^*\langle j|\langle f_l|b_kH'(t)|D_2^M(t)\rangle$ to express them in terms of the variational parameters, which yields

$$\langle j|\langle f_l|\dot{D}_2^M(t)\rangle = \sum_{n=1}^{M}\sum_{i=1}^{N_S}\left(a_{nj} + A_{nj}\sum_{p=1}^{N}f_{lp}^*\dot{f}_{np}\right)\mathcal{S}_{ln}, \tag{A7}$$

$$\sum_{j=1}^{N_S}A_{lj}^*\langle j|\langle f_l|b_k|\dot{D}_2^M(t)\rangle = \sum_{n=1}^{M}\sum_{j,i=1}^{N_S}\left(A_{lj}^*a_{nj}f_{nk} + A_{lj}^*A_{nj}\sum_{p=1}^{N}\left(\delta_{k,p} + f_{lp}^*f_{nk}\right)\dot{f}_{np}\right)\mathcal{S}_{ln}, \tag{A8}$$

$$[\vec{I}_j]_l = \langle j|\langle f_l|H'(t)\left|D_2^M(t)\right\rangle = \sum_{n=1}^{M}\sum_{i=1}^{N_S}\langle j|H_S(t)|i\rangle A_{ni}\mathcal{S}_{ln} + \sum_{n=1}^{M}\sum_{i=1}^{N_S}\sum_{p=1}^{N}\frac{g_p}{2}A_{ni}(\langle j|V_p^\dagger|i\rangle e^{-i\omega_p t}f_{np} + \langle j|V_p|i\rangle e^{i\omega_p t}f_{lp}^*)\mathcal{S}_{ln}, \tag{A9}$$

$$\begin{aligned}[\vec{I}_f]_{lk} = &\sum_{j=1}^{N_S}A_{lj}^*\langle j|\langle f_l|b_kH'(t)\left|D_2^M(t)\right\rangle = \sum_{n=1}^{M}\sum_{j,i=1}^{N_S}A_{lj}^*\langle j|H_S(t)|i\rangle A_{ni}\mathcal{S}_{ln}f_{nk} + \sum_{n=1}^{M}\sum_{j,i=1}^{N_S}\sum_{p=1}^{N}\frac{g_p}{2}A_{lj}^*A_{ni}[\langle j|V_p^\dagger|i\rangle e^{-i\omega_p t}f_{np}f_{nk} \\ &+ \langle j|V_p|i\rangle e^{i\omega_p t}(\delta_{p,k} + f_{lp}^*f_{nk})]\mathcal{S}_{ln}, \end{aligned} \tag{A10}$$

where $[\vec{I}_f]_{lk}$ is viewed as a column vector with its component position being specified by l and k. By substituting these quantities into Eqs. (17) and (18), we can rewrite the equations of motion in a matrix form:

$$i\begin{pmatrix} \mathcal{S} & & & & \mathcal{C}^{(1)} \\ & \mathcal{S} & & & \mathcal{C}^{(2)} \\ & & \ddots & & \vdots \\ & & & \mathcal{S} & \mathcal{C}^{(N_S)} \\ \mathcal{C}^{(1)\dagger} & \mathcal{C}^{(2)\dagger} & \cdots & \mathcal{C}^{(N_S)\dagger} & \mathcal{D} \end{pmatrix}\begin{pmatrix} \vec{a}_1 \\ \vec{a}_2 \\ \vdots \\ \vec{a}_{N_S} \\ \vec{F} \end{pmatrix} = \begin{pmatrix} \vec{I}_1 \\ \vec{I}_2 \\ \vdots \\ \vec{I}_{N_S} \\ \vec{I}_f \end{pmatrix}, \tag{A11}$$

where $\mathcal{S}$ is an $M \times M$ matrix whose elements are $\mathcal{S}_{ln}$, $\vec{a}_j = (a_{1j}, a_{2j}, \ldots, a_{Mj})^T$, $\vec{F}$ is a vector whose components are given by f_{np}, $\mathcal{C}^{(j)}$ is an $M \times MN$ matrix whose elements are given by

$$\mathcal{C}^{(j)}_{l,np} = A_{nj}\mathcal{S}_{ln}f^*_{lp}, \tag{A12}$$

and $\mathcal{D}$ is an $MN \times MN$ matrix whose matrix elements are

$$\mathcal{D}_{lk,np} = \sum_{j=1}^{N_S} A^*_{lj}A_{nj}(\delta_{k,p} + f^*_{lp}f_{nk})\mathcal{S}_{ln}. \tag{A13}$$

To perform a numerical simulation, we first numerically solve the matrix equation (A11) as a set of linear equations to obtain the values of $\vec{a}_j$ and $\vec{F}$. The former can be combined with Eq. (A6) to calculate the derivatives of A_{nj}. The latter are just the derivatives of f_{np}. On obtaining the derivatives of A_{nj} and f_{np}, we can use the fourth-order Runge-Kutta algorithm to update the variational parameters.

[1] M. O. Scully and M. S. Zubairy, *Quantum Optics* (Cambridge University Press, Cambridge, 1997).

[2] C. Cohen-Tannoudji, J. Dupont-Roc, and G. Grynberg, *Atom-Photon Interactions: Basic Processes and Applications* (Wiley-VCH, Weinheim, 2004).

[3] N. Rivera and I. Kaminer, Light-matter interactions with photonic quasiparticles, Nat. Rev. Phys. **2**, 538 (2020).

[4] C. L. Degen, F. Reinhard, and P. Cappellaro, Quantum sensing, Rev. Mod. Phys. **89**, 035002 (2017).

[5] A. Karnieli, S. Tsesses, R. Yu, N. Rivera, Z. Zhao, A. Arie, S. Fan, and I. Kaminer, Quantum sensing of strongly coupled light-matter systems using free electrons, Sci. Adv. **9**, eadd2349 (2023).

[6] J. Joo, W. J. Munro, and T. P. Spiller, Quantum metrology with entangled coherent states, Phys. Rev. Lett. **107**, 083601 (2011).

[7] S.-Y. Bai and J.-H. An, Floquet engineering to overcome no-go theorem of noisy quantum metrology, Phys. Rev. Lett. **131**, 050801 (2023).

[8] F. Pirmoradian and K. Mølmer, Aging of a quantum battery, Phys. Rev. A **100**, 043833 (2019).

[9] Y.-Y. Zhang, T.-R. Yang, L. Fu, and X. Wang, Powerful harmonic charging in a quantum battery, Phys. Rev. E **99**, 052106 (2019).

[10] A. Crescente, M. Carrega, M. Sassetti, and D. Ferraro, Charging and energy fluctuations of a driven quantum battery, New J. Phys. **22**, 063057 (2020).

[11] M. B. Arjmandi, A. Shokri, E. Faizi, and H. Mohammadi, Performance of quantum batteries with correlated and uncorrelated chargers, Phys. Rev. A **106**, 062609 (2022).

[12] D. Braak, Integrability of the Rabi model, Phys. Rev. Lett. **107**, 100401 (2011).

[13] D. Braak, Q.-H. Chen, M. T. Batchelor, and E. Solano, Semiclassical and quantum Rabi models: In celebration of 80 years, J. Phys. A **49**, 300301 (2016).

[14] Q. Xie, H. Zhong, M. T. Batchelor, and C. Lee, The quantum Rabi model: Solution and dynamics, J. Phys. A **50**, 113001 (2017).

[15] F. Yoshihara, T. Fuse, S. Ashhab, K. Kakuyanagi, S. Saito, and K. Semba, Superconducting qubit-oscillator circuit beyond the ultrastrong-coupling regime, Nat. Phys. **13**, 44 (2017).

[16] S. Felicetti, E. Rico, C. Sabin, T. Ockenfels, J. Koch, M. Leder, C. Grossert, M. Weitz, and E. Solano, Quantum Rabi model in the Brillouin zone with ultracold atoms, Phys. Rev. A **95**, 013827 (2017).

[17] D. Lv, S. An, Z. Liu, J.-N. Zhang, J. S. Pedernales, L. Lamata, E. Solano, and K. Kim, Quantum simulation of the quantum Rabi model in a trapped ion, Phys. Rev. X **8**, 021027 (2018).

[18] A. F. Kockum, A. Miranowicz, S. D. Liberato, S. Savasta, and F. Nori, Ultrastrong coupling between light and matter, Nat. Rev. Phys. **1**, 19 (2019).

[19] P. Forn-Díaz, L. Lamata, E. Rico, J. Kono, and E. Solano, Ultrastrong coupling regimes of light-matter interaction, Rev. Mod. Phys. **91**, 025005 (2019).

[20] A. Le Boité, Theoretical methods for ultrastrong light-matter interactions, Adv. Quantum Technol. **3**, 1900140 (2020).

[21] F. Yoshihara, Y. Nakamura, F. Yan, S. Gustavsson, J. Bylander, W. D. Oliver, and J.-S. Tsai, Flux qubit noise spectroscopy using Rabi oscillations under strong driving conditions, Phys. Rev. B **89**, 020503(R) (2014).

[22] C. Deng, J.-L. Orgiazzi, F. Shen, S. Ashhab, and A. Lupascu, Observation of Floquet states in a strongly driven artificial atom, Phys. Rev. Lett. **115**, 133601 (2015).

[23] G. Romero, D. Ballester, Y. M. Wang, V. Scarani, and E. Solano, Ultrafast quantum gates in circuit QED, Phys. Rev. Lett. **108**, 120501 (2012).

[24] Y. Song, J. P. Kestner, X. Wang, and S. Das Sarma, Fast control of semiconductor qubits beyond the rotating-wave approximation, Phys. Rev. A **94**, 012321 (2016).

[25] E. K. T. Irish and A. D. Armour, Defining the semiclassical limit of the quantum Rabi Hamiltonian, Phys. Rev. Lett. **129**, 183603 (2022).

[26] J. Hausinger and M. Grifoni, Qubit-oscillator system: An analytical treatment of the ultrastrong coupling regime, Phys. Rev. A **82**, 062320 (2010).

[27] C. J. Gan and H. Zheng, Dynamics of a two-level system coupled to a quantum oscillator: Transformed rotating-wave approximation, Eur. Phys. J. D **59**, 473 (2010).

[28] Y.-Y. Zhang, Generalized squeezing rotating-wave approximation to the isotropic and anisotropic Rabi model in the ultrastrong-coupling regime, Phys. Rev. A **94**, 063824 (2016).

[29] L. Cong, X.-M. Sun, M. Liu, Z.-J. Ying, and H.-G. Luo, Polaron picture of the two-photon quantum Rabi model, Phys. Rev. A **99**, 013815 (2019).
[30] M. Werther and F. Grossmann, Including temperature in a wavefunction description of the dynamics of the quantum Rabi model, J. Phys. A **51**, 014001 (2018).
[31] M. Werther and F. Grossmann, The Davydov D1.5 ansatz for the quantum Rabi model, Phys. Scr. **93**, 074001 (2018).
[32] Z.-M. Li, D. Ferri, and M. T. Batchelor, Nonorthogonal-qubit-state expansion for the asymmetric quantum Rabi model, Phys. Rev. A **103**, 013711 (2021).
[33] Q.-H. Chen, C. Wang, S. He, T. Liu, and K.-L. Wang, Exact solvability of the quantum Rabi model using Bogoliubov operators, Phys. Rev. A **86**, 023822 (2012).
[34] J. H. Shirley, Solution of the Schrödinger equation with a Hamiltonian periodic in time, Phys. Rev. **138**, B979 (1965).
[35] S.-I. Chu and D. A. Telnov, Beyond the Floquet theorem: Generalized Floquet formalisms and quasienergy methods for atomic and molecular multiphoton processes in intense laser fields, Phys. Rep. **390**, 1 (2004).
[36] G. Engelhardt, S. Choudhury, and W. V. Liu, Unified light-matter Floquet theory and its application to quantum communication, Phys. Rev. Res. **6**, 013116 (2024).
[37] Y. Zhao, K. Sun, L. Chen, and M. Gelin, The hierarchy of Davydov's ansätze and its applications, Wiley Interdiscip. Rev.: Comput. Mol. Sci. **12**, e1589 (2022).
[38] Y. Zhao, The hierarchy of Davydov's ansätze: From guesswork to numerically "exact" many-body wave functions, J. Chem. Phys. **158**, 080901 (2023).
[39] L. Wang, Y. Fujihashi, L. Chen, and Y. Zhao, Finite-temperature time-dependent variation with multiple Davydov states, J. Chem. Phys. **146**, 124127 (2017).
[40] M. Werther and F. Großmann, Apoptosis of moving nonorthogonal basis functions in many-particle quantum dynamics, Phys. Rev. B **101**, 174315 (2020).
[41] Y. Yan, Spontaneous emission spectrum from a V-type artificial atom in a strong-coupling regime: Dark lines and line narrowing, Phys. Rev. A **108**, 043712 (2023).
[42] J. Frenkel, *Wave Mechanics* (Oxford University Press, Oxford, 1934).
[43] M. J. Everitt, W. J. Munro, and T. P. Spiller, Quantum-classical crossover of a field mode, Phys. Rev. A **79**, 032328 (2009).
[44] S. Stenholm, Saturation effects in RF spectroscopy. I. General theory, J. Phys. B **5**, 878 (1972).
[45] Z. Lü and H. Zheng, Effects of counter-rotating interaction on driven tunneling dynamics: Coherent destruction of tunneling and Bloch-Siegert shift, Phys. Rev. A **86**, 023831 (2012).
[46] R. Guccione-Gush and H. P. Gush, Two-level system in a bichromatic field, Phys. Rev. A **10**, 1474 (1974).
[47] T.-S. Ho and S.-I. Chu, Semiclassical many-mode Floquet theory. II. Non-linear multiphoton dynamics of a two-level system in a strong bichromatic field, J. Phys. B **17**, 2101 (1984).
[48] W. M. Ruyten, Harmonic behavior of the multiple quantum resonances of a two-level atom driven by a fully-amplitude-modulated field, Phys. Rev. A **40**, 1447 (1989).
[49] W. M. Ruyten, Resonance behavior of a two-level quantum system in a two-frequency field, Phys. Rev. A **46**, 4077 (1992).
[50] Y. Yan, Z. Lü, L. Chen, and H. Zheng, Multiphoton resonance band and Bloch-Siegert shift in a bichromatically driven qubit, Adv. Quantum Technol. **6**, 2200191 (2023).
[51] R. H. Dicke, Coherence in spontaneous radiation processes, Phys. Rev. **93**, 99 (1954).
[52] D. Zueco and J. García-Ripoll, Ultrastrongly dissipative quantum Rabi model, Phys. Rev. A **99**, 013807 (2019).